

Separate print taken from:

Nachrichten aus dem Karten- und Vermessungswesen, Reihe II: Übersetzungen — Heft Nr. 36

Paper presented to the Symposium of Commission III

International Society for Photogrammetry, Moscow, USSR, 1978

Printed and published by Institut für Angewandte Geodäsie, Frankfurt a. M. 1978

DK 519.233.4/.5:[528.113:528.7]

Auto- and Cross-Correlation of Image Coordinates

(with 7 Figures and 2 Tables)

By *F. Ackermann and M. Schilcher, Stuttgart*

SUMMARY: Two series of wide-angle- and of super-wide-angle photographs of the testfield Rheidt are used to determine empirically the correlation of image coordinates within a photograph and between different photographs. The results show strong correlations which remain constant between different photographs even. The correlations depend on the systematic image errors, after compensation of which they are reduced considerably to rather small magnitudes.

RÉSUMÉ: Deux séries de photographes grand-angulaires et ultra-grand-angulaires du champs d'essai Rheidt sont utilisées pour déterminer empiriquement des corrélations entre des coordonnées de l'image et aussi des images différentes. Les résultats démontrent des corrélations fortes et constantes même entre des images différentes. Elles sont dépendentes des erreurs systématiques des images. Conséquemment elles sont fortement réduites par leur compensation.

ZUSAMMENFASSUNG: Anhand zweier Serien von Weitwinkel- und Überweitwinkel-aufnahmen des Testfeldes Rheidt werden die Korrelationsverhältnisse der Bildkoordinaten im Bild und zwischen verschiedenen Bildern empirisch untersucht. Im Ergebnis werden starke und auch zwischen verschiedenen Bildern konstante Korrelationen festgestellt, die von den systematischen Bildfehlern abhängen und die nach der zusätzlichen Korrektur der systematischen Bildfehler stark zurückgehen.

1 Introduction

1.1 During the last two decades analytical photogrammetry has made great progress by operating directly with the bundle of rays as fundamental geometrical unit, determined by image points and the interior orientation of a photograph. Aerial triangulation, cadastral photogrammetry or other applications referring to point determination have carried the development which has been truly spectacular, both in terms of accuracy and economy.

When analyzing the development we can identify the simultaneous treatment of the overlapping photographs of a block as the main feature which constitutes the progress. Apart from the improved quality of hardware (cameras, film, comparators) the progress has mainly been due to block adjustment as such, whilst the state of correction of image coordinates has remained on the conventional level.

For some time the attention has been directed towards systematic image errors. The methods of testfield-calibration and of selfcalibration have succeeded to determine and to correct for systematic deformation of the bundle of rays and to

effectively increase the resulting accuracy. It constitutes a major step, that the geometry of the bundle of rays has been refined beyond the conventional state of a priori correction for regular lens distortion and refraction.

Correction of systematic image errors relates to the functional description of the bundle of rays as basic geometrical unit. By comparison, little thought has been given, up to now, to the stochastic properties of image coordinates. They are still treated as uncorrelated observations and often of equal weight even, although it is very well known, in qualitative terms, that the image coordinates of a photograph, and likewise also between different photographs, are highly correlated.

Thus, the stochastic behaviour of image coordinates remains a problem to be investigated. The investigation is due, in first instance, as a principal matter of the theory of errors of photographs. It is also due in view of the possibility of still increasing and of predicting the accuracy of analytical photogrammetry by considering correlation.

1.2 At Stuttgart University an investigation has been set up in order to assess accuracy and correlation of image coordinates, both within photographs and between adjacent photographs, and also between photographs of different spacings on a film roll. The investigation was repeated for different levels of correction of systematic image errors, as variances and covariances are expected to depend very much on the remaining systematic image errors.

Very little is known about the physical processes causing the stochastic properties of aerial photographs up to film development and measurement of image coordinates. It seemed not feasible, therefore, to approach the problem theoretically. Hence the investigation is empirical, by studying the image errors of a number of actual photographs of the camera-calibration-testfield Rheidt¹⁾ near Bonn. The empirical approach implies some problems, it also limits the direct validity of the results to the data of the experiment. On the other hand it depends very little on prefixed theoretical assumptions.

2 Material and procedure

2.1 The testfield Rheidt covers a flat area of 2 km x 2 km. It has 41 signalized points arranged in a grid pattern, each point with 2 auxiliary signals of about 5 m distance. All points are determined geodetically with standard errors in plan and height of < 1 cm.

Aerial photography was taken with two RMK cameras at photo-scale 1 : 10,500:

- wide angle (w.a.), $f = 153$ mm (Pleogon A), in 1969 by Häussermann company, Waiblingen
- super wide angle (s.w.a.), $f = 85$ mm (Pleogon AS), in 1975 by Hansa Luftbild, Münster.

1) We acknowledge the cooperation of the Photogrammetric Institute of the University of Bonn (Prof. Kupfer).

In each case the area was covered, in 4 flight directions, by 20 short strips of 3 photographs each, with 60 % forward overlap, forming 2 stereo pairs. Thus each mission gave 60 photographs, of which 20 frames completely cover the test area. The photographs used do not form an uninterrupted series of frames on the film. There are varying numbers of frames inbetween, because partly 90 % overlap was actually taken and the cameras were not switched off immediately.

2.2 Glass diapositives of the photographs were measured with a stereo-comparator PSK 2 by *M. Schilcher*. The instrument was used as a monocomparator, with non-stereoscopic, binocular observation. The photographs were measured twice, with resulting standard measuring errors of the means of double measurements of $1.0 \mu\text{m}$ (w.a.) and $1.2 \mu\text{m}$ (s.w.a.) respectively.

2.3 The comparator measurements (double measurements reduced to the mean) were transformed to the calibrated image coordinate system by affine transformation (w.a.) and by similarity transformation (s.w.a.). Preliminary tests have shown that the affine transformation was significant only for the wide-angle photography.

Together with the image transformation the image coordinates were corrected for lens distortion, refraction and earth curvature in the usual way (radial symmetrical with regard to the principal point). Only the correction of the lens distortion was somewhat refined, by interpolation between the 4 half-diagonals (radial correction as function of azimuth).

2.4 For each image a spatial resection was computed using all signalized points as control points. Thus the central photographs of the strips rely on about $41 \times 3 = 123$ control points, all other photographs on about $23 \times 3 = 69$ control points. For the resection computations the image coordinates, after correction for a priori distortion, were introduced as uncorrelated observations of weight 1 (weight matrix $\mathbf{P} =$ unit matrix \mathbf{I}).

The residual errors at the control points gave standard errors $\sigma_0 = 3.5 \mu\text{m}$ (w.a.) and $\sigma_0 = 5.3 \mu\text{m}$ (s.w.a.) of image coordinates, see table 1. Those values reflect the absolute accuracy after resection and indicate the general high quality of the material. The residual errors v_x, v_y at the control points can be taken, in first approximation, as "true errors" of the image coordinates, although they are slightly affected and correlated by the preceding resection process. They serve as basic data for the error investigation.

Table 1 – Accuracy results after spatial resection

camera	images	control points	resection, standard errors of image coord. without / with corr. for syst. errors		accuracy improvement	systematic errors r.m.s.-values	
			σ_0 [μm]	σ_0 [μm]		s_x [μm]	s_y [μm]
WA RMK A 15/23	60	69/123	3.5	3.0	1.2	1.7	1.6
SWA RMK A 8.5/23	60	69/123	5.3	4.1	1.3	4.0	2.3

2.5 As all observations refer to known ground control points it was possible, after the resection, to determine the systematic image errors (see section 3.2).

Each photograph was corrected for the average image errors of the complete set. Thereafter new resections were computed, giving again residual errors at the control points. The standard errors changed to $\sigma_0 = 3.0 \mu\text{m}$ (w.a.) and $\sigma_0 = 4.1 \mu\text{m}$ (s.w.a.), see table 1.

3 Subdivision in local fields and determination of systematic errors

3.1 Establishing accuracy and correlation of image coordinates as function of the location of points in the photographs is the primary aim of the investigation. As no explicit functional relationship is envisaged, and because of the actual arrangement of the points in the testfield the area was subdivided in 41 separate fields. By superimposing all 60 photographs all image errors became related to the respective fields in the photographs. Maintaining the local fields with respect to the camera-(image-) system, all image points thus related to a field were considered representative for the field in question, independent of their actual location within the field, see fig. 1. Hence the errors $(v_x, v_y)_{ijk}$ of all image points i of the images k were used to established variances and covariances for the various fields j .

3.2 The correction for systematic image errors (see section 2.5) was made per field, by subtracting the arithmetic mean (in x and y) of all errors in the field. With such constant corrections per field the previous image coordinates were reduced and new resections computed. The new sets of residual image errors were used for a second error analysis in the same way as the previous one.

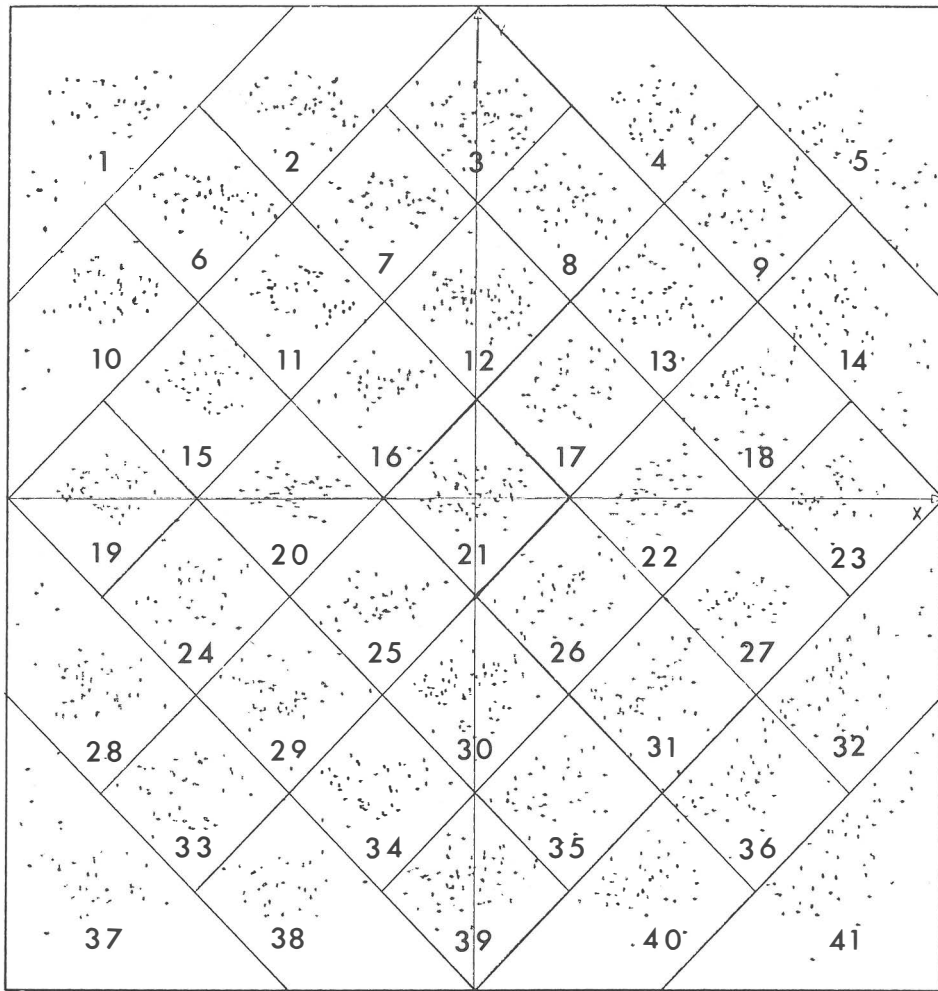


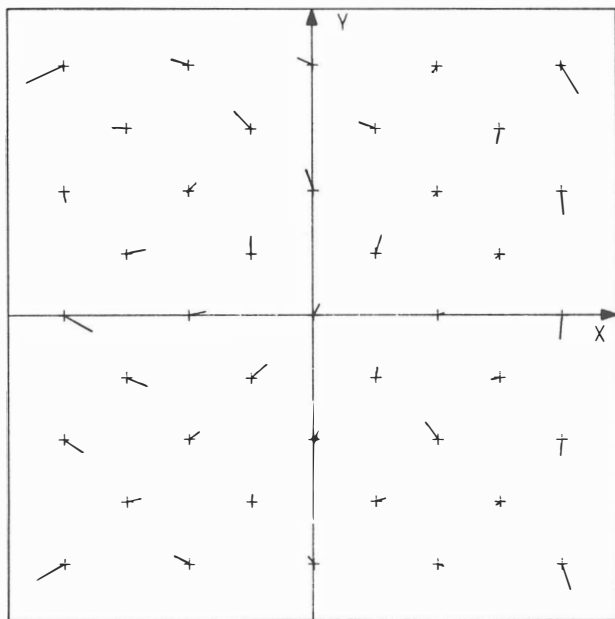
Fig. 1 – Superposition of photographs and subdivision of the reference image area in 41 local fields

3.3 The systematic image errors, determined according to 3.2, are displayed in the vector diagrams of fig. 2. The r.m.s. vector magnitudes are $1.7 \mu\text{m}$ (w.a.) and $3.3 \mu\text{m}$ (s.w.a.). The maximum vectors reach values of $4.7 \mu\text{m}$ (w.a.) and $8.7 \mu\text{m}$ (s.w.a.) respectively. Correction of the systematic image errors improved the accuracy of resected points by factors of 1.2 (w.a.) and 1.3 (s.w.a.) respectively, see table 1.

The magnitudes of the systematic errors agree in general with the results of previous investigations. Especially the systematic deformation of the wide-angle photographs appears quite continuous and smooth. Contrary to that the systematic deformation of the s.w.a.-photographs shows some discontinuities. In particular the 9 standard points do not represent other points very well. The interior part of the vector field appears to be separated from the marginal parts.

10 wide angle

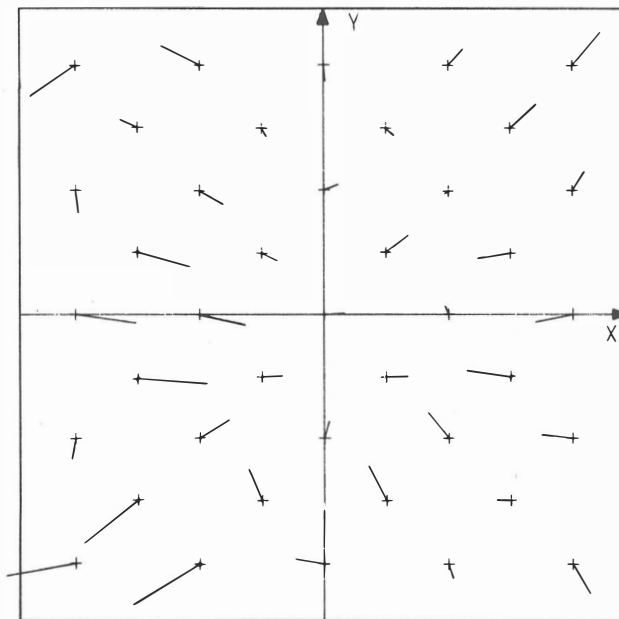
RMK A 15/23



5 μm

super wide angle

RMK A 8.5/23



5 μm

Fig. 2 – Vector diagrams of systematic image errors

4 Assessment of correlation

With each of the available sets of data the correlation analysis distinguished 3 different cases:

- variances and covariances of image coordinates within the photographs
- correlation between adjacent, overlapping photographs
- correlation between (non-overlapping) photographs as function of relative spacing on the roll of film.

The subdivision of the correlation analysis was made for computational reasons, and also in view of the 3 main levels of dealing with photographs in practice (single photograph, pair, and block of photographs).

4.1 Variances and covariances within the photograph

The experimental data allowed to establish a complete variance-covariance matrix of the image coordinates of 41 points, each representing its local field within the image area. The result is a 82 x 82 symmetrical matrix, partitioned for auto- and cross-correlation in x and y , see fig. 3.

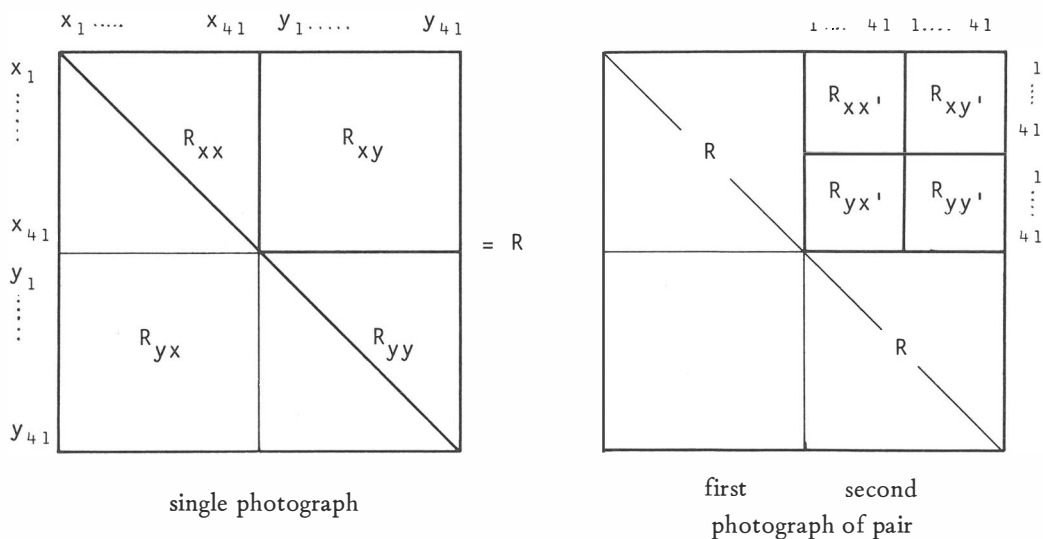


Fig. 3 – Partitioning of correlation matrices (single photograph and pair of photographs)

For the empirical estimation of variances and covariances the residual errors ν^x and ν^y at the image coordinates (after the spatial resections) are considered sufficient estimates of the “true” image errors. If they may be treated as sufficiently independent

samples the variances and covariances can be computed as the mean values of the respective error-products. Consider the individual points i (1, 2, 3) within a field j (1 . . . 41) of a photograph k (1 . . . 60), then we obtain the

– v a r i a n c e s of the x - and y -image coordinates of the field j :

$$(\sigma_x^2)_j = \frac{1}{n_j} \sum_k \sum_i (v_{ijk}^x)^2 \quad (1)$$

$$(\sigma_y^2)_j = \frac{1}{n_j} \sum_k \sum_i (v_{ijk}^y)^2$$

n_j = total number of points in field j

– c o v a r i a n c e s between the x - and y -image coordinates of fields j and j' :

$$\begin{aligned} \sigma_{x_j x_{j'}} &= \frac{1}{n_{jj'}} \sum_k \left\{ \sum_i \left[\sum_{i'} (v_{ijk}^x v_{i'j'k}^x) \right] \right\} (j' \neq j) \\ \sigma_{y_j y_{j'}} &= \frac{1}{n_{jj'}} \sum_k \left\{ \sum_i \left[\sum_{i'} (v_{ijk}^y v_{i'j'k}^y) \right] \right\} (j' \neq j) \\ \sigma_{x_j y_{j'}} &= \frac{1}{n_{jj'}} \sum_k \left\{ \sum_i \left[\sum_{i'} (v_{ijk}^x v_{i'j'k}^y) \right] \right\} \end{aligned} \quad (2)$$

$n_{jj'}$ = number of products involved

From the covariances correlation coefficients were derived ($r_{jj'} = \sigma_{jj'} / \sqrt{\sigma_j^2 \cdot \sigma_{j'}^2}$) and presented as correlation matrix R , with the auto- and cross-correlation submatrices R_{xx} , R_{yy} and R_{xy} , see fig. 3. Each coefficient was tested for significance, on the 95 % level (two-sided).

4.2 Correlation between adjacent, overlapping photographs

The correlation between adjacent, overlapping photographs is of interest with regard to the accuracy of stereo-models. Therefore, all pair-combinations were used to establish covariances and correlation-coefficients between the x and y image coordinates in all combinations of the 41 fields between adjacent photographs (see fig. 3).

If we indicate the second (mate-)photograph by $k' = k + 1$, and refer to the points and fields of the k' photograph with i' and j' , then the formulae (2) can be extended for the computation of c o v a r i a n c e s :

$$\sigma_{x_j x_{j'}} = \frac{1}{n_{jj'}} \sum_k \left\{ \sum_i \left[\sum_{i'} (v_{ijk}^x v_{i'j'k'}^x) \right] \right\} \quad (3)$$

similarly for $\sigma_{y_j y_{j'}}$, $\sigma_{x_j y_{j'}}$ and also $\sigma_{y_j x_{j'}}$.

The summation index k now runs over the total number of pairs (k, k') , and $n_{jj'}$ represents the total number of products involved.

Attention is drawn to the fact that the photographs forming stereopairs are in fact separated by several frames on the film which were not included in the investigation. Thus, the index $k' = k + 1$ relates to the photographs actually used.

With forward overlap of 60 % in a strip a photograph k still overlaps with the photograph $k' = k + 2$ for 20 %. Therefore the covariances and correlations were also computed between the overlapping photographs k and $k' = k + 2$, using again formulae (3). For sake of completeness also the full 82 x 82 covariance-matrices were established.

4.3 Correlation between non-overlapping photographs as a function of spacing on the roll of film

The assessment of covariances between different photographs, based on formulae (3), can be extended to arbitrary values $k' = k + s$, s expressing the spacing between frames k and k' on the roll of film. With the testfield photographs s goes up to 167 and 277, respectively, as the 60 w.a. (s.w.a.) photographs were selected from 168 (278) actual exposures taken.

Correlation matrices for all available spacings s were computed, on the basis of formulae (3). However, the number of fields considered was reduced to the 9 standard fields which are essential for aerial triangulation (field no. 1, 3, 5, 19, 21, 23, 37, 39, 41, see fig. 1). Also, the elements of the main diagonal only were computed, as this is sufficient to construct the complete covariance matrix in case needed.

4.4 Additional remarks

It must be mentioned that the theoretical basis of the computational procedure applied is valid only approximately. The effects have been investigated, especially the question of correlation between the image coordinates due to the orientation procedure. Also the effects of varying numbers of points per field and the rank-defects of some semi-definite-covariance matrices were studied. It has been confirmed that the theoretical effects of the approximations disappear almost completely. Hence, the resulting correlations, as presented here, can be considered valid in first approximation.

5 Results

5.1 Presentation of the results

The correlation computations, as described under section 4.1–4.3, were performed for both the w.a.- and the s.w.a.-material as well as for the 2 levels of correction of systematic image errors.

The immediate results are available in form of covariance-matrices and of matrices of correlation-coefficients. They are too voluminous to be presented in this paper. Therefore, only a verbal assessment of the results can be given, and examples of individual results are presented graphically.

5.2 Distribution of variances of image coordinates

The average values of the standard errors of image coordinates amount for w.a. (s.w.a.) photographs to $3.5 \mu\text{m}$ ($5.2 \mu\text{m}$) without and to $3.0 \mu\text{m}$ ($4.1 \mu\text{m}$) with additional correction of systematic image errors, see table 2. The standard coordinate errors for the 41 fields range

for w.a.	from $2.5 \mu\text{m}$ to $6.5 \mu\text{m}$ without	}	additional correction of systematic image errors
	from $2.1 \mu\text{m}$ to $4.3 \mu\text{m}$ with		
for s.w.a.	from $2.9 \mu\text{m}$ to $10.9 \mu\text{m}$ without		
	from $2.7 \mu\text{m}$ to $6.2 \mu\text{m}$ with		

Fig. 4 shows in graphical form the variations of the standard errors of image coordinates within the image area. It is noticeable that the state of correction of systematic image errors influences the variances and their distribution in the image plane. Correction of systematic image errors does reduce the absolute magnitudes of the variances, for s.w.a. in particular. Moreover, the distributions become considerably more homogeneous.

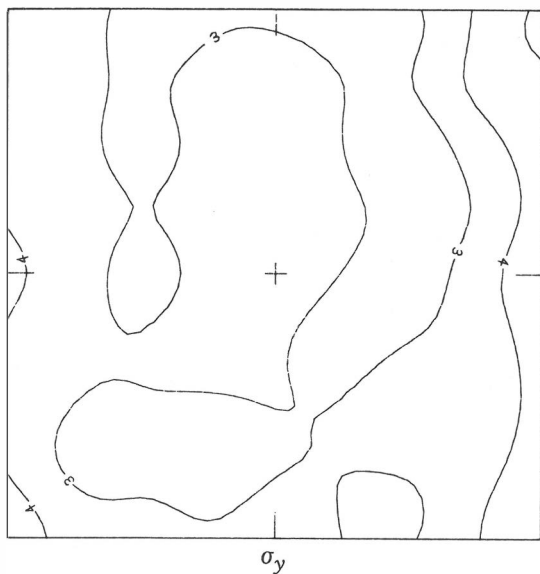
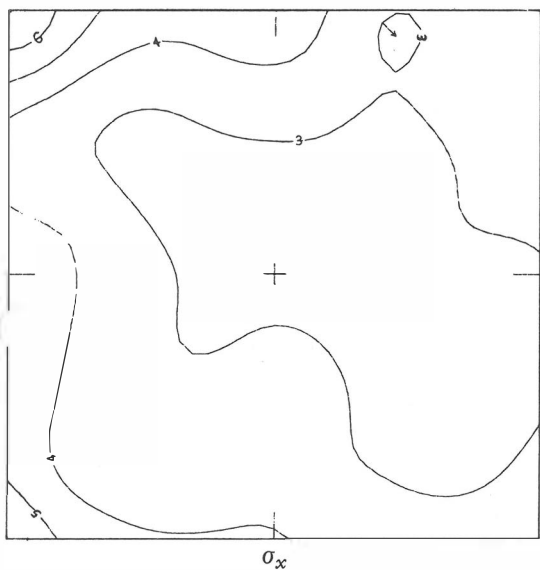
The variances are dependent on the location within the photograph. However, there is no marked radial symmetrical relation. In fact, the symmetry relations are noticeably different in x and y . By which physical features (camera, film) such effects are caused can here, of course, not be established on the basis of the available data.

Table 2 – Accuracy results of image coordinates and percentage of significant correlation coefficients

version with / without correction of systematic errors	standard errors of image coordinates				significant correlation coefficients, in % of total number			
	r.m.s.-values		min./max. values		r_{xx}	r_{yy}	r_{xy}	average
	σ_x [μm]	σ_y [μm]	σ_x [μm]	σ_y [μm]				
w.a. without	3.5	3.4	2.5/ 6.5	2.5/5.0	62.4	71.8	66.6	66.8
w.a. with	3.0	3.0	2.1/ 4.3	2.2/3.8	55.5	58.2	55.1	56.0
s.w.a. without	5.7	4.7	3.2/10.9	2.9/7.0	76.8	58.7	66.9	67.3
s.w.a. with	4.1	4.0	2.7/ 6.2	2,7/6,1	41.2	36.0	37.6	38.1

wide angle

without correction of systematic image errors



with correction of systematic image errors

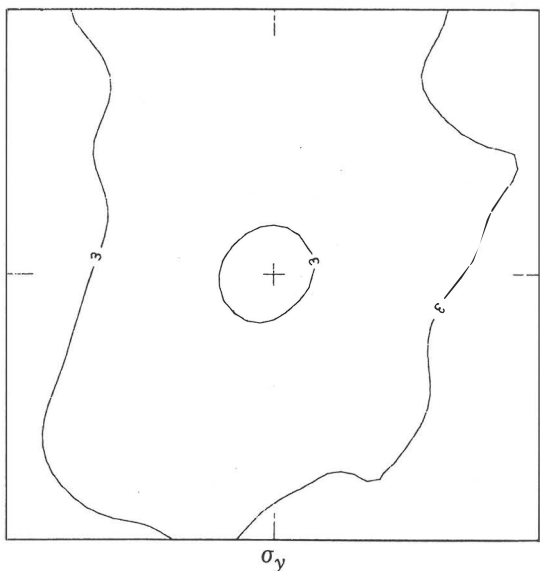
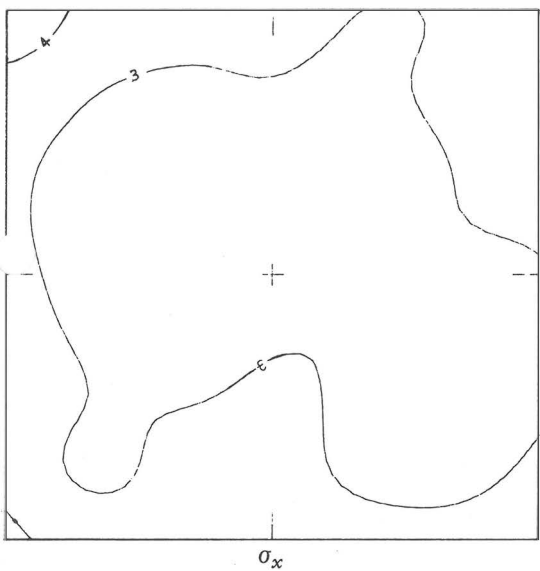
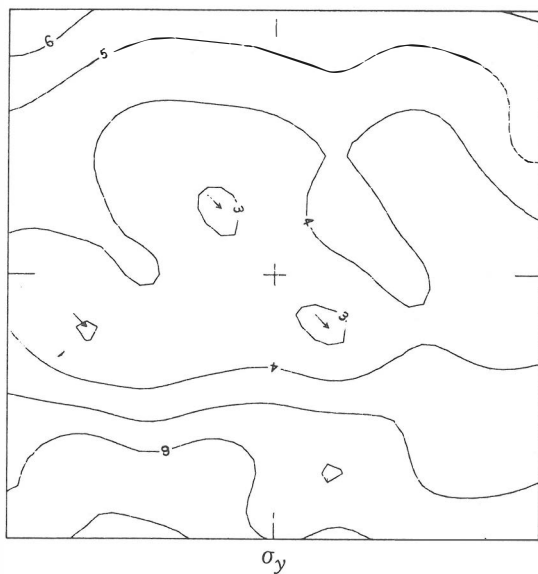
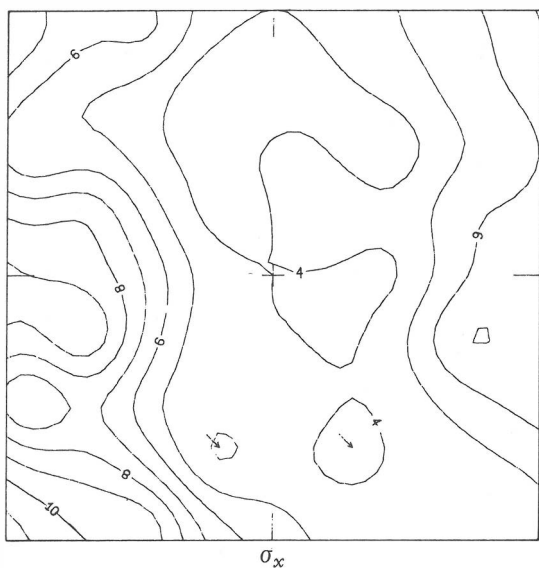


Fig. 4a – Distribution of standard errors of image coordinates in the image plane (in μm , interval $1 \mu\text{m}$)

super wide angle
without correction of systematic image errors



with correction of systematic image errors

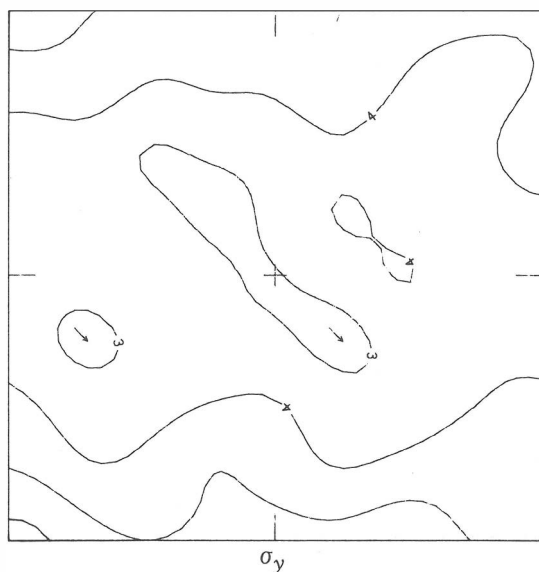
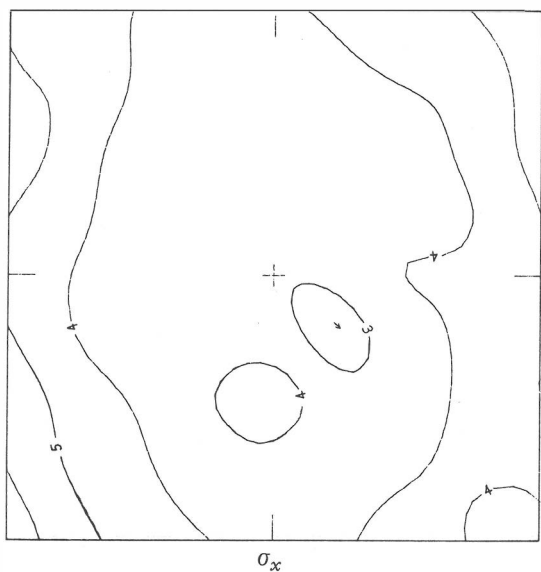


Fig. 4b – Distribution of standard errors of image coordinates in the image plane (in μm , interval $1 \mu\text{m}$)

5.3 Correlation within the photograph

Table 2 also records the percentages of all computed correlation coefficients, which are significantly different from 0, referring to correlation within the photograph. Without corrections of systematic errors an average of 67 % of the computed correlation coefficients for auto- and cross-correlation in the photograph is significant. After the correction of systematic errors that percentage is reduced to 56 % (w.a.) and 38 % (s.w.a.) respectively. Those values indicate, that before additional correction of systematic image errors the correlation within the photograph is rather high, correlation coefficients of ± 0.6 are regularly obtained and superseded. After additional correction of systematic image errors the absolute values of the correlation coefficients drop considerably. Apart from the immediate surrounding of a point the absolute correlation values hardly exceed 0.4 any more (see fig. 5).

Such results indicate, that most of the initial high correlations are caused by the systematic image errors. This is confirmed by the graphical plotting of curves of equal correlation between a point and all other image points, see fig. 6. The iso-lines of 0-correlation follow in most cases closely the course of the 0-lines of the x - and y -component of the systematic image errors.

5.4 Correlation between different photographs

As far as correlation between different photographs is concerned the 2 cases of overlapping and non-overlapping photographs need not be distinguished. The examples displayed in fig. 5, 6, and 7 are representative for the general result. Before correction of systematic image errors the correlations within the photograph, between adjacent photographs, and between photographs of large spacing are very much alike. The correlation coefficients reach absolute magnitudes of 0.6 and more. The most important result is, however, that those large values of correlation are maintained throughout the film. The values do not drop or tend towards 0-values. In view of the results of section 5.3 the obvious explanation is once more, that the high correlation is caused by systematic image errors. As long as they are not accounted for, systematic image errors remain rather stable through a series of frames. Therefore the correlations display the same behaviour.

After correction of systematic image errors the remaining correlation between different photographs drop considerably, mostly to absolute values of less than 0.4. With large spacings between the photographs the correlation coefficients fall more and more below the level of significance, see fig. 7. This effect reflects in first instance the decreasing number of common photographs involved. It may also indicate the expected effect of decreasing correlation as a property of the underlying stochastic process.

5.5 Some conclusions

The results of the investigation show in first instance a remarkably constant pattern of correlation between arbitrary photographs of a roll of film. This

points to the strong interdependence between systematic image errors and correlation. As long as systematic errors are not accounted for, image coordinates within the photograph and between different photographs are highly correlated. The actual pattern of magnitudes and signs depends on the remaining systematic errors. It is virtually independent of the spacing between photographs. Also w.a.- and s.w.a.-photographs display in general similar behaviour, although the numerical values are different.

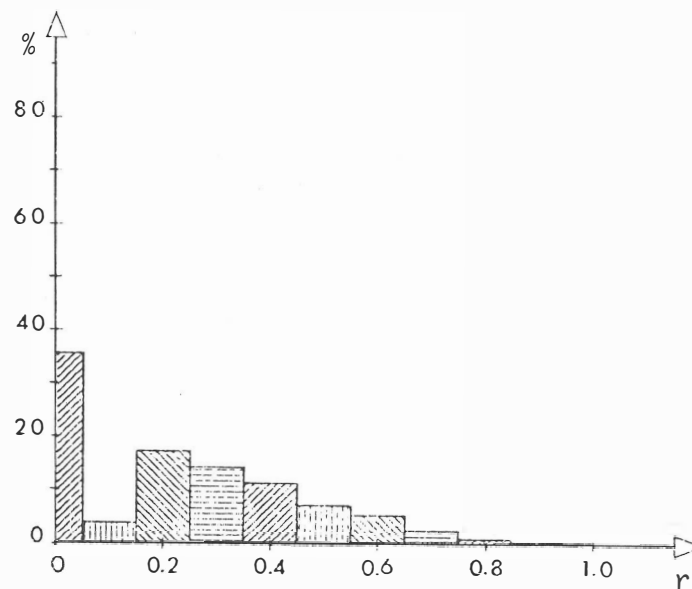
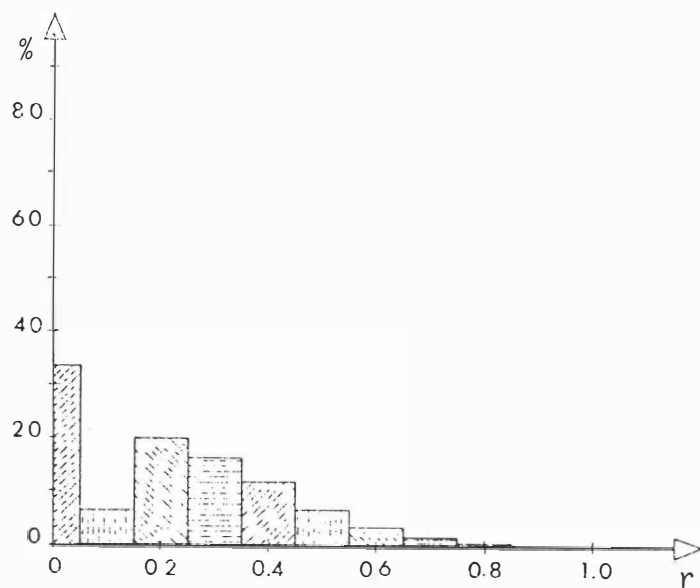
After correction of systematic errors (on the basis of test-field-calibration or of selfcalibration) the remaining correlation between image coordinates of a photograph or of different photographs is considerably reduced, and the values of quite a number of correlation coefficients drop below the threshold of significance. The coefficients which remain significant have mostly absolute values of only 0.2–0.4.

Considering those results it can be concluded that the determination of systematic image errors is (and remains) of major importance in order to reach maximum accuracy. Beyond the systematic image errors the truly stochastic properties of photographs are surprisingly small, small enough to be neglected in most practical cases (of block-triangulation for instance).

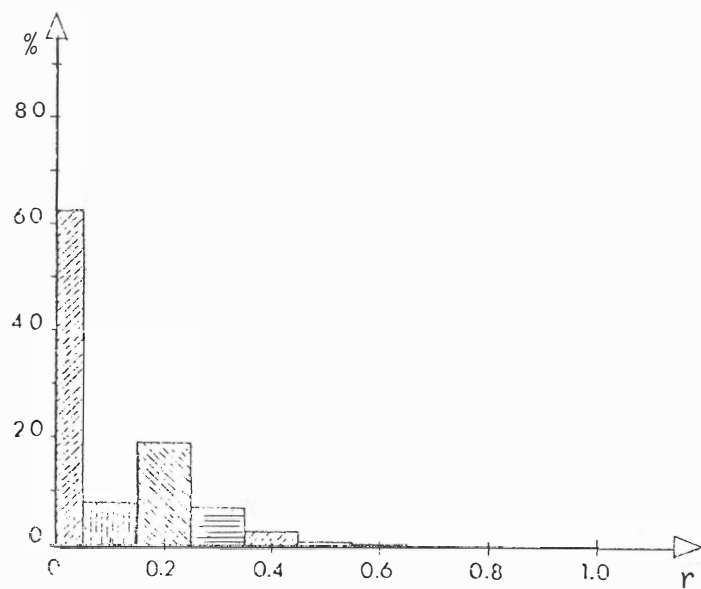
The consideration of correlation does become essential, however, whenever systematic image errors cannot be determined beyond the conventional state of a priori knowledge. This is the case with single model restitution or with small blocks.

We intend to continue the research by studying such cases in more detail, based on the results of the present investigation.

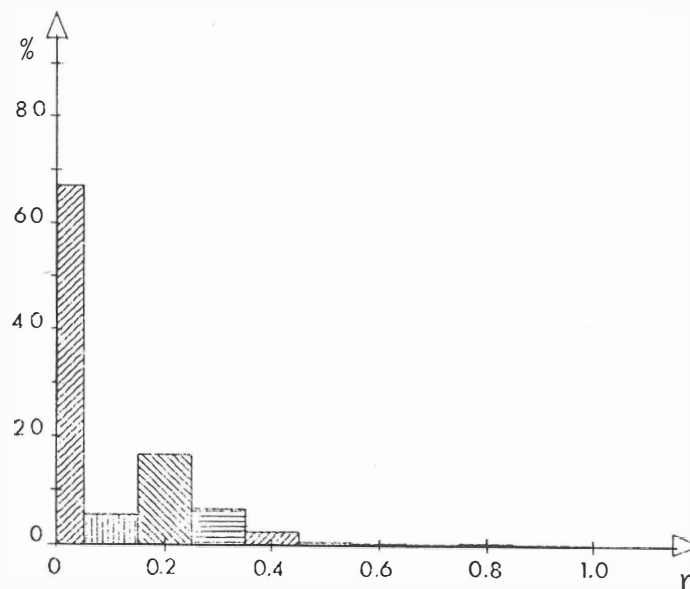
without correction of systematic errors



with correction of systematic errors



correlation
within the photograph



correlation
between adjacent photographs
($p = 60\%$)

Fig. 5 – Examples of histograms of correlation coefficients (s.w.a.)

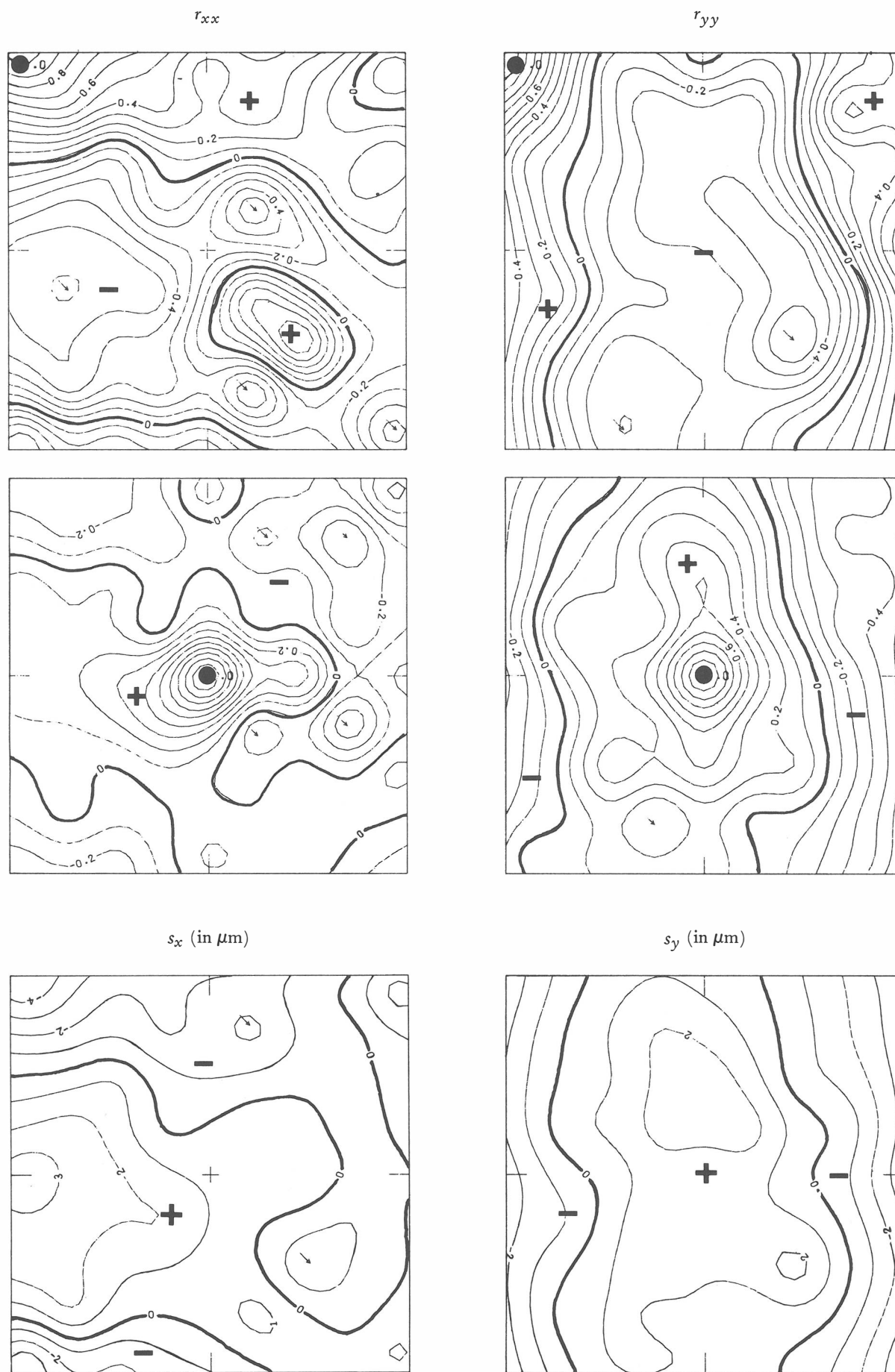


Fig. 6 – Two examples of auto-correlation without correction of systematic image errors (w.a., interval $\Delta r = 0.1$); and comparison with systematic image errors